SCIENCE CHINA
Earth Sciences

•REVIEW•

September 2021 Vol.64 No.9: 1481–1491
https://doi.org/10.1007/s11430-020-9788-0

Gold solubility in silicate melts and fluids: Advances from high-pressure and high-temperature experiments

Xingcheng LIU[1,2,3*], Ting XU[1,2,3], Xiaolin XIONG[1,2,3], Li LI[1,2] & Jianwei LI[4]

[1] *State Key Laboratory of Isotope Geochemistry, Guangzhou Institute of Geochemistry, Chinese Academy of Sciences, Guangzhou 510640, China;*
[2] *CAS Center for Excellence in Deep Earth Science, Guangzhou 510640, China;*
[3] *College of Earth and Planetary Sciences, University of Chinese Academy of Sciences, Beijing 100049, China;*
[4] *Faculty of Earth Resources, China University of Geosciences, Wuhan 430074, China*

Received October 23, 2020; revised April 30, 2021; accepted May 10, 2021; published online June 25, 2021

Abstract The solubility of Au in silicate melts and fluids governs the enrichment and migration of Au during the formation of magmatic-hydrothermal Au deposits. Large Au deposits require vast amounts of Au to migrate from the upper mantle-lower crust to the shallow crust, and high Au solubility in magma and hydrothermal fluid facilitates the formation of Au-rich magma and fluid in the crust and mantle source and efficient transport. This paper reviews recent high-pressure and high-temperature experimental studies on Au species in magmas and hydrothermal fluids, the partitioning behavior of Au between silicate melts and fluids, and the effects of temperature, pressure, oxygen fugacity, sulfur fugacity, silicate melt composition, and volatiles (H_2O, CO_2, chlorine, and sulfur) on the solubility of Au in magma. We show that the solubility of Au in magma is largely controlled by the volatiles in the magma: the higher the content of reduced sulfur (S^{2-} and HS^-) in the magma, the higher the solubility of Au. Under high-temperature, high-pressure, H_2O-rich, and intermediate oxygen fugacity conditions, magma can dissolve more reduced sulfur species, thus enhancing the ability of the magma to transport Au. If the ore-forming elements of the Au deposits in the North China Craton originate from mantle-derived magmas and fluids, we can conclude, in terms of massive Au migration, that these deep Au-rich magmas might have been generated under H_2O-rich and moderately oxidized conditions (S^{2-} coexists with S^{6+}). The big mantle wedge beneath East Asia was metasomatized by melts and fluids from the dehydration of the Early Cretaceous paleo-Pacific stagnant slab, which not only caused thinning of the North China Craton, but also created physicochemical conditions favorable for massive Au migration.

Keywords Magmatic-hydrothermal gold deposits, Gold solubility, Sulfur solubility, Volatiles, High-pressure and high-temperature experiments

Citation: Liu X, Xu T, Xiong X, Li L, Li J. 2021. Gold solubility in silicate melts and fluids: Advances from high-pressure and high-temperature experiments. Science China Earth Sciences, 64(9): 1481–1491, https://doi.org/10.1007/s11430-020-9788-0

1. Introduction

Gold is valuable and has long been of great interest to economic geologists. There are various types of Au deposits, including deposits where the formation is not directly related to magmatic activity, such as orogenic Au deposits formed during orogenesis (Mao et al., 2002; Chen et al., 2009; Groves and Santosh, 2016), and deposits closely related to magmatic processes, such as porphyry Au-Cu deposits, epithermal Au deposits, Au-rich volcanogenic massive sulfide (VMS) deposits, and Carlin-type Au deposits (Walshe and Cleverley, 2009; Heinrich and Candela, 2014; Zhu et al., 2015). The ore-forming processes of magmatic-hydrothermal Au deposits require magma and

* Corresponding author (email: liuxingcheng@gig.ac.cn)

subsequent fluid exsolution to transport large amounts of Au from deep sources to shallow mineralization sites. Specifically, in the magmatic processes associated with ore formation, Au needs to be extracted from the lithospheric mantle by the magma, which crosses the mantle-crust boundary, intrudes upward, and undergoes complex magmatic and hydrothermal evolution to form Au-bearing fluids to precipitate and mineralize Au in favorable tectonic regions. In these processes, the solubility of Au in volatile-rich magmas controls the Au transport, i.e., high Au solubility facilitates the transport of large amounts of Au. In addition, high Au solubility in magma will reduce the partition coefficient of Au between sulfide and magma (Li et al., 2019), which will facilitate the formation of Au-rich magma in the source region. The solubility of Au in magmas and fluids thus governs the enrichment and migration of Au during ore-forming processes. Constraining the physicochemical factors controlling the solubility of Au in magmas (silicate melts) and fluids can therefore help improve our understanding of the favorable conditions for Au-rich magma formation and Au transport. With the development of Laser-Ablation Inductively-Coupled-Plasma Mass Spectrometry (LA-ICP-MS), the precise determination of trace amounts of Au in experimental products has become feasible. Thus, numerous high-pressure and high-temperature experimental studies have been carried out in recent years to investigate the solubility and partitioning behavior of Au in melts and fluids (Borisov and Palme, 1996; Loucks and Mavrogenes, 1999; Frank et al., 2002; Hanley et al., 2005; Simon et al., 2005, 2007; Bell et al., 2009, 2011; Botcharnikov et al., 2010, 2011; Jégo et al., 2010, 2016; Zajacz et al., 2010, 2012, 2013; Jégo and Pichavant, 2012; Li and Audétat, 2013; Li et al., 2019; Pokrovski et al., 2015; Brenan et al., 2016; Sullivan et al., 2018; Audétat, 2019). In this paper, we review the state of the art of high-pressure and high-temperature experimental studies on Au solubility in silicate melts and fluids, and combine recent experimental results to investigate the effects of physicochemical factors such as temperature, pressure, oxygen fugacity (fO_2), sulfur fugacity (fS_2), and magma composition (including volatiles) on Au solubility in magma. Based on the results, we summarize the physicochemical conditions favorable for the generation of Au-rich magma that form magma-hydrothermal Au deposits, providing an experimental constraint on the genesis of magmatic-hydrothermal Au deposits, especially for decratonic Au deposits.

2. Geochemical behavior of Au in fluids

The valence, species, and geochemical behavior of Au in fluids have been widely studied; in particular, the results of *in situ* observations are based on fluid-related studies. In the ore-forming processes of magmatic-hydrothermal deposits, decompression during magma ascent and crystallization of magma can lead to fluid exsolution. Understanding the geochemical behavior of Au in fluids can help us better understand the factors controlling the solubility of Au in magma. Therefore, this review will first introduce the valence and species of Au prevalent in fluids and the role of magmatic-hydrothermal fluid in the extraction, enrichment, and migration of Au.

2.1 Valence and speciation of Au in fluids

The common valence states of Au are Au^0, Au^{1+}, and Au^{3+}. Native gold (Au^0) is very inert and usually does not react with acid or alkali and is resistant to corrosion. However, Au^0 can be oxidized by nitric acid and other strong oxidizing agents, forming Au^{3+}. For example, Au^0 can be dissolved in aqua regia (a mixture of nitric acid and hydrochloric acid in a molar ratio of 1:3): Au^0 is oxidized to Au^{3+}, which then complexes with chlorine ions to form $AuCl^{4-}$. In magmatic-hydrothermal systems, Au mostly occurs as Au^{1+} (Pokrovski et al., 2009, 2015; Seward et al., 2014; Brugger et al., 2016; Sullivan et al., 2018).

According to Pearson's (1963) soft-hard acid-base theory, the electron acceptor is an acid and the electron donor is the base. Au^{1+} and Au^{3+} are soft ions that are more likely to complex with soft ligands. At room temperature, Au^{1+} tends to form stable complexes with HS^-, $S_2O_3^{2-}$, CN^-, and SCN^- (Williams-Jones et al., 2009). Because Au^{1+} and Au^{3+} are not stable in pure water, Au in fluids is predominantly transported in complexes with Cl and S (Williams-Jones et al., 2009; Heinrich and Candela, 2014; Liu et al., 2014; Seward et al., 2014; Pokrovski et al., 2015). As shown in Table 1, when the temperature is less than 350°C, the most important ligand for Au is HS^- (Seward, 1973; Williams-Jones et al., 2009). As the temperature increases, the dielectric constant of H_2O decreases, which favors electrostatic interactions and allows Au^{1+} to form stable bonds with harder bases, such as Cl^- and OH^-. During the hydrothermal stage of the ore-forming process (~<600°C), Au is mainly transported in the form of complexes with HS^- under moderately acidic conditions (Williams-Jones et al., 2009; Seward et al., 2014). X-ray absorption near edge spectroscopy (XANES) studies further indicate that $Au(HS)_2^-$ is the predominant complex in neutral S-bearing hydrothermal fluids (Pokrovski et al., 2009).

Fluids with high salinity (Cl-rich) are usually acidic because of charge balance effects (Heinrich and Candela, 2014). In acidic S-bearing fluids, the stability of HS^- decreases because of the lower pH, and although $AuHS^0$ can be formed, the Au solubility decreases in hydrothermal fluids

Table 1 Species of Au in hydrothermal fluids

Temperature	Acidic conditions	Neutral to acidic conditions
<350°C	AuHS	$Au(HS)_2^-$
350–600°C	$AuCl_2^-$	$Au(HS)_2^-$, ± $Au(HS)S_3^-$, ± AuOH

(Pokrovski et al., 2009). Thus, $AuCl_2^-$ dominates in fluids under acidic (and oxidizing) conditions (e.g., most Cu-Au porphyry-type deposit systems) (Heinrich and Candela, 2014; Pokrovski et al., 2015). However, experimental studies suggest that under high-pressure and high-temperature conditions (e.g., at 1000°C and 150 MPa), HS^- may also replace Cl^- as the most important ligand for Au complexation in the fluid (Zajacz et al., 2010). These stable Au complexes in hydrothermal fluids may also play an important role in magmatic systems, although no reliable *in situ* observations have been reported.

In addition to the formation of complexes with Cl^- and HS^- in hydrothermal fluids, S_3^- has recently been recognized as a notable complex for the transport of Au under high-pressure and high-temperature conditions (200–700°C; ~3.0 GPa) (Pokrovski and Dubrovinsky, 2011; Pokrovski et al., 2015). S_3^- has the following properties: (1) higher solubility in fluids (>1000 ppm, 1 ppm=1 mg kg^{-1}); (2) stability under weakly acidic to neutral conditions (pH=3–7); and (3) stability at oxygen fugacities, where S^{2-} or SO_2 coexist with HS^- (Pokrovski et al., 2015). Because S_3^- decomposes into S^{2-} and S^{6+} during cooling, the presence of S_3^- in fluids can only be detected in *in situ* diamond anvil cell high-pressure experiments (Pokrovski and Dubrovinsky, 2011; Colin et al., 2020). There is no evidence that S_3^- is stable in magmatic systems at high temperatures. As a multivalent element, S can occur in different oxidation states in fluids under various fO_2 conditions. For example, the melts and fluids derived from subducting slabs are believed to be oxidized, and S^{4+} (SO_2) may be more stable than S^{2-} (H_2S). In magmatic-hydrothermal systems under oxidizing conditions, in addition to S^{2-}, S^{4+} (SO_2 or HSO_3^- and SO_3^{2-}) may also complex with Au and influence Au transport. Because SO_2 is "harder" than H_2S at high temperatures, it is more likely to bind with Au (Pokrovski et al., 2009). However, there is no direct evidence (e.g., XANES) to support the existence of Au-S^{4+} complexes (von der Heyden, 2020). It should be noted that CO_2 is common in fluid inclusions in Au deposits. It is generally believed that this CO_2 does not directly bind with Au to form complexes, but may control fluid pH and induce fluid exsolution (Pokrovski et al., 2013; Bodnar et al., 2014). In summary, the behavior of Au in fluids is dominated by volatiles (particularly Cl and S), and the Au complexes in fluids vary under different temperature, pressure, fO_2, and pH conditions.

2.2 Solubility of Au in fluids and Au partitioning between fluid and melt

Fluid inclusions trapped in the shallow crust (<150 MPa, ~6 km) can be divided based on salinity into a low-to-moderate salinity and low-density vapor phase (H_2O±HCl ±H_2S±CO_2) and a high-salinity and high-density brine phase (H_2O-NaCl±KCl) (Loucks and Mavrogenes, 1999; Pettke et al., 2012; Pokrovski et al., 2013; Heinrich and Candela, 2014; Audétat, 2019). In the case of coexisting vapor and brine phases, Au preferentially partitions into the higher salinity brine phase over the vapor phase (partition coefficients are listed in Table 2). For example, Simon et al. (2005) studied the partition coefficients of Au between fluid and silicate melt (D_{Au}) in a NaCl-KCl-$FeCl_2$-HCl-H_2O system at a temperature of 800°C and pressures of 110–145 MPa, and obtained $D_{Au}^{vapor/silicate\ melt}$=8–72 and $D_{Au}^{brine/silicate\ melt}$=56–100. The $D_{Au}^{vapor/brine}$ increased from 0.21 to 0.72 with increasing salinity of the vapor phase. However, unlike Cu, the Au content did not further increase with increasing Cl content in the fluid. For instance, in the experiments without S but rich in Cl (NaCl =20–70 wt%) at 150 MPa and 600–800°C, the solubility of Au in the fluid decreased from several thousand ppm to a few ppm as the Cl content (salinity) increased (Hanley et al., 2005). In addition to composition, temperature also affects the solubility of Au in fluids. In an S-free and Cl-rich hydrothermal fluid, the solubility of Au can increase by one order of magnitude for every 100°C increment in temperature when the salinity is constant (Hanley et al., 2005).

Fluids associated with Au deposit formation often contain S and Cl (Seo et al., 2009; Seward et al., 2014), including HS^- as an important ligand for complexation with Au. Loucks and Mavrogenes (1999) found that the solubility of Au in Cl-bearing fluids increased with increasing fugacity of H_2S by synthesizing fluid inclusions (550–725°C, 100–400 MPa), revealing the complexation of HS^- with Au. However, other studies suggest that the enhanced Au content in fluids with increased S content may be related to S_3^- (Pokrovski et al., 2015). In contrast, it has also been found that at 800°C and 120 MPa, S does not affect the partitioning of Au between low-salinity vapor phases (2 wt% NaCl) and rhyolitic silicate melts, with $D_{Au}^{vapor/silicate\ melt}$=12±0.3 for the S-bearing system and $D_{Au}^{fluid/silicate\ melt}$=15±2.5 for the S-free system (Simon et al., 2007). It seems that the role of S in fluids for Au dissolution and partitioning behavior is much less than that of Cl (Table 2). It is worth noting that because S is redox-sensitive, its valence is controlled by fO_2. Under reduced conditions, S occurs as S^{2-}; under oxidized conditions, S is present as S^{6+}, and S_3^- is stable at intermediate fO_2. S^{6+} does not complex with Au, and the experiments with S-

Table 2 Partition coefficients of Au between fluid and silicate melt[a)]

Starting materials	P (GPa)	T (°C)	Oxygen fugacity (ΔFMQ)	Sulfur fugacity (log fS_2)	$D_{Au}^{vapor/silicate\ melt}$	$D_{Au}^{brine/silicate\ melt}$	Reference
Haplogranite*	0.1–0.15	800	0.8	–	8–72	56–100	Simon et al., 2005
Haplogranite**	0.12	800	0.8	−3	12±0.3	–	Simon et al., 2007
Haplogranite*	0.12	800	0.8	–	15±2.5	–	Simon et al., 2007

a) *, Cl-bearing and S-free system; **, Cl- and S-bearing system

bearing but low-salinity fluids are basically at fO_2 of the Ni-NiO buffer, in which S is present mainly as S^{2-}. Thus, the effect of S_3^- on $D_{Au}^{fluid/silicate\ melt}$ is not well constrained. Furthermore, the available $D_{Au}^{fluid/silicate\ melt}$ is still limited at pressures greater than 0.5 GPa, suggesting that the extraction efficiency of deep fluids on Au is not clear.

3. Solubility of Au in magma

Ore-forming elements such as Au and Cu, and fluids in magmatic-hydrothermal deposits usually originate from mantle-derived mafic magmas (Mungall, 2002; Audétat and Simon, 2012; Richards, 2015; Zhu et al., 2015; Wang et al., 2020, 2021). The abundance of Au is 3 ppb(1 ppb=1 μg kg^{-1}) in the crust and 1–2 ppb in mantle source regions (Wang et al., 2020, 2021). Thus, more than 1000-fold enrichment is required to reach a grade of 3–30 ppm in Au deposits (Yang et al., 2003). According to the $D_{Au}^{fluid/silicate\ melt}$ mentioned in Section 2.2, the extraction process through magmatic-hydrothermal fluid exsolution can only elevate the Au content by approximately 1–2 orders of magnitude, implying that the magma needs to be enriched in Au by 1–2 orders of magnitude relative to the mantle source.

As a chalcophile element, Au has low solubility in silicate minerals and Fe-Ti oxides (less than 0.1 ppm in olivine and clinopyroxene at 1000°C; approximately 2 ppm in magnetite at 800°C), and thus Au is primarily stored in sulfides in the source (Bell et al., 2011; Kiseeva et al., 2017; Simon et al., 2017; Li et al., 2019). If sulfide is retained in the source during partial melting or fractional crystallization of the ascending magma, it is crucial to enhance the solubility of Au in the magma to form Au-rich magma and Au deposits.

Numerous high-pressure and high-temperature experimental studies have been conducted in recent years to investigate the conditions favorable for the generation of Au-rich magmas (Borisov and Palme, 1996; Frank et al., 2002; Simon et al., 2005, 2007; Bell et al., 2009, 2011; Botcharnikov et al., 2010, 2011; Jégo et al., 2010, 2016; Zajacz et al., 2010, 2012, 2013; Jégo and Pichavant, 2012; Li and Audétat, 2013; Li et al., 2019; Brenan et al., 2016; Sullivan et al., 2018). However, most previous experiments were conducted under upper crustal pressure conditions (<0.4 GPa), and high-pressure experiments at lower crustal conditions are limited (see Table 3; previous experimental conditions and results are summarized). Here, we systematically evaluated the effects of temperature, pressure, melt composition, oxygen fugacity, sulfur fugacity, and volatiles on the dissolution of Au in magma, combined with our new experimental results under lower crustal conditions (1.0 GPa and 950°C; see the text section in the Appendix for details of the experiments, https://link.springer.com).

3.1 Effects of temperature and pressure

The effects of temperature and pressure on the solubility of Au in magma are limited if the impact of volatiles is excluded (Zajacz et al., 2013; Brenan et al., 2016). High-pressure and high-temperature experimental studies have shown that the solubility of Au in magma increases with increasing temperature (Figure 1). For example, the solubility of Au in rhyolitic silicate melts increases by 1–2 orders of magnitude as the temperature increases from 800°C to 1000°C (Zajacz et al., 2013). Compared to the temperature, the effect of pressure was much smaller. Previous experimental results demonstrated that the effect of pressure on Au solubility is almost negligible at pressures ranging from 0.1 MPa to 18 GPa (Brenan et al., 2016). However, magmas associated with magmatic-hydrothermal deposits are usually volatile-rich, and temperature and pressure have a significant influence on the solubility of volatiles in magma. Therefore, the role of volatiles needs to be considered to understand the temperature and pressure dependence of the solubility of Au in magma (see discussion in Section 3.4).

3.2 Effect of silicate melt composition

For a volatile-free system (200 MPa, 1000–1030°C, fO_2= FMQ, FMQ is the fayalite-magnetite-quartz fO_2 buffer), the solubility of Au in the magma was found to be very low and the effect of the silicate melt composition weak, which was 56±12 ppb, 70±18 ppb, and 31±7 ppb in basaltic, andesitic, and dacitic melts, respectively (Zajacz et al., 2013). In addition, the solubility of Au increased with decreasing degree of silicate melt polymerization (i.e., higher NBO/T, lower content of network-forming ions such as Si, Al, and Fe^{3+}) and decreasing aluminum saturation index (Zajacz et al., 2013).

Table 3 Summary of experimental conditions and results for the Au solubility in silicate melts[a)]

Starting materials	*P*	*T* (°C)	Oxygen fugacity (ΔFMQ)	Sulfur fugacity (log fS_2)	H_2O in melt (wt%)	S in melt (ppm)	Cl in melt (wt%)	Au in melt (ppm)	Reference
Anorthite-diopside	1 atm	1300–1480	4.9–6.2	–	dry	S-free	Cl-free	31.3–51.6	Borisov and Palme, 1996
Anorthite-diopside	1 atm	1300–1480	−4.2–3.0	–	dry	S-free	Cl-free	0.3–11.7	Borisov and Palme, 1996
Haplogranite	0.1 GPa	800	0.8	–	3.5–7.9	S-free	0.07–0.29	~1	Frank et al., 2002
Haplogranite	0.1–0.15 GPa	800	0.8	–	5.1–7.7	S-free	0.2	~0.5	Simon et al., 2005
Haplogranite	0.12 GPa	800	0.8	−3	5.1–6.2	164–189	0.1	0.36–1.1	Simon et al., 2007
Haplogranite	0.12 GPa	800	0.8	–	5.5–6.5	S-free	0.1	1.1–4.7	Simon et al., 2007
Haplogranite	0.15 GPa	800	0.8	−5.16–−0.19	7.3–8.5	74–245	0.09~0.21	0.02–0.65	Bell et al., 2009
Basalt to rhyolite	0.2 GPa	800–1030	0	−3.03–−1.74	5.9–7.3	115–670	Cl-free	0.06–4.3	Zajacz et al., 2013
Basalt to rhyolite	0.2 GPa	800–1030	0	–	4.8–7.6	S-free	Cl-free	0.02–0.13	Zajacz et al., 2013
Andesite	0.2 GPa	1000	0.2	–	5.5	S-free	Cl-free	0.04	Zajacz et al., 2012
Andesite	0.2 GPa	1000	−0.9–2.5	–	5.1–6.8	S-free	0.5~12.3	0.04–0.24	Zajacz et al., 2012
Andesite	0.2 GPa	1000	−0.9–2.5	–	4.6–6.7	67–2019	Cl-free	0.22–1.54	Zajacz et al., 2012
Andesite	0.2 GPa	1000	0.2–4.7	–	4.2–6.6	207–1915	1.8~12.9	0.65–4.57	Zajacz et al., 2012
Andesite	0.2 GPa	1000	0.4–7.4	–	4.2–4.7	S-free	Cl-free	0.15–3.85	Sullivan et al., 2018
Andesite	0.2 GPa	1000	0.4–7.4	–	4.7–4.8	S-free	0.4	0.15–9.8	Sullivan et al., 2018
Andesite	0.2 GPa	1000	0.4–2.5	–	4.1–5.1	170–3000	Cl-free	0.31–0.56	Sullivan et al., 2018
Basalt	0.2 GPa	1000	0	–	6.6–7.3	S-free	1.2~1.9	0.1–0.49	Bell et al., 2011
Basalt	0.2 GPa	1000	4	–	6.4–8.1	S-free	1.2~2.1	0.64–4.9	Bell et al., 2011
Andesite to basalt	0.2 GPa	1050	−0.4–2.9	−0.69–1.97	2.6–4.7	390–6020	Cl-free	0.25–7.97	Botcharnikov et al., 2011
Rhyodacite to andesite	0.2 GPa	1050	0.8	–	5.8–6.8	S-free	0.2~1.0	0.28–0.86	Botcharnikov et al., 2010
Rhyodacite to andesite	0.2 GPa	1050	0.8	–	2.5–6.6	20–410	Cl-free	0.24–2.47	Botcharnikov et al., 2010
Dacite to diorite	0.4 GPa	1000–1090	−1–3.2	–	4.1–9.2	S-free	Cl-free	0.03–0.24	Jégo et al., 2010
Dacite to diorite	0.4 GPa	995–1090	−0.4	–	5.9–8.0	548–957	Cl-free	1.2–4.3	Jégo et al., 2010
Dacite to diorite	0.4 GPa	995–1000	−0.6–4.1	−3.76–3.16	3.4–8.0	256–2422	Cl-free	0.25–5.16	Jégo and Pichavant, 2012
Dacite to diorite	0.9–1.4 GPa	950–1000	0–0.8	–	5.4–11.7	S-free	Cl-free	0.07–0.23	Jégo et al., 2016
Dacite to diorite	0.9–1.4 GPa	975–1000	0–0.8	0.55–3.84	8.2–14.8	261–3865	Cl-free	0.3–47	Jégo et al., 2016
Rhyolite to andesite	0.5–3.0 GPa	950–1040	−1.7–2.7	−2.17–2.08	0–12.3	48–5536	Cl-free	0.01–11	Li et al., 2019

a) The solubility of Au in the alloy was obtained in Zajacz et al. (2012, 2013) (0.99 and 0.98 for Au activity, respectively), which is similar to the solubility of pure Au

It should be noted that ore-forming magmas associated with Au deposits are usually alkali-rich (Na and K) (Mungall, 2002; Yang et al., 2003; Richards, 2015). Although the silicate melts in our experiments contained up to 13–16 wt% K, the solubility of Au in the melts was not significantly higher than that of the basaltic to rhyolitic melt compositions in previous experiments. This suggests that the silicate melt composition itself has limited influence, i.e., whether or not the magma is alkali-rich, does not directly affect the solubility of Au and the ability of the magma to transport Au. This implies that the correlation between K-rich and Au-rich magmas may not be directly related to the alkali content, but is more likely due to the generation of alkali-rich magmas being influenced by the degree of partial melting and volatile content of the source, which control the Au content in magma. Therefore, during the formation of magmatic-hydrothermal deposits, the changes in temperature, pressure, and melt composition through magma evolution have a greater influence on the solubility of volatiles in magma and less on the solubility of Au.

3.3 Effect of oxygen fugacity

It is believed that Au is predominantly present as Au^{1+} in magma and can be dissolved in magma as oxide ($AuO_{0.5}$) (Brenan et al., 2016; Sullivan et al., 2018):

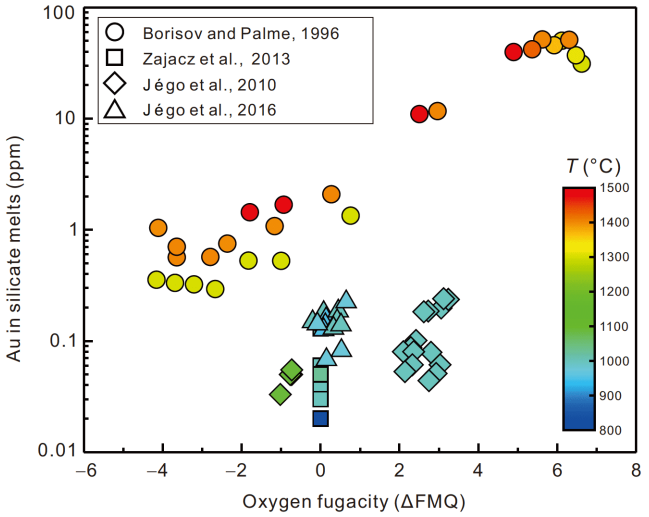

Figure 1 Solubility of Au in volatile-free silicate melts as a function of oxygen fugacity and temperature. Without volatiles, Au is present as $AuO_{0.5}$ in silicate melts. Therefore, the solubility of Au is higher at elevated oxygen fugacities at the same temperature. Under similar redox conditions, the solubility of Au in silicate melts increases with increasing temperature. Details on the experimental conditions are listed in Table 3.

$$Au(metal)+0.25O_2(gas)=AuO_{0.5}(melt), \quad (1)$$

Reaction (1) shows that an increase in fO_2 will increase the $AuO_{0.5}$ content in the silicate melt. In the absence of volatiles such as S and Cl, and at constant temperature and pressure, the solubility of Au in magma increases with increasing fO_2 as long as the fO_2 is above FMQ−4 (Figure 1). The solubility of Au in volatile-free basaltic melts was found to increase from 1.4 to 11 ppm with fO_2 increasing from FMQ−2 to FMQ+2 at ambient pressure and 1480°C (Borisov and Palme, 1996). Similarly, with fO_2 increasing from ~FMQ to FMQ+7 at 200 MPa and 1000°C, the solubility of Au in hydrous andesitic melts (S- and Cl-free) increased from 0.1 to 3.8 ppm (Sullivan et al., 2018). For ore-forming magma, owing to the relatively low solubility of $AuO_{0.5}$, it is unlikely that massive amounts of Au were transported in the form of oxides, but rather as complexes with ligand anions provided by volatiles.

3.4 Effect of volatiles

As shown in Table 3, the addition of volatiles enhances the solubility of Au in magmas at similar temperatures, pressures, melt compositions, and fO_2. Volatiles contained in the ore-forming magmas include H_2O, S, CO_2, fluorine, and Cl (Audétat and Lowenstern, 2014). Similar to the behavior of Au in fluids, the solubility of Au in magma is essentially influenced by Cl and S (Botcharnikov et al., 2010; Zajacz et al., 2010, 2012, 2013; Sullivan et al., 2018):

$$Au(metal)+1/xMeCl_x(melt)+0.25O_2(gas) = AuCl(melt)+1/xMeO_{x/2}(melt), \quad (2)$$

$$Au(metal)+FeS(melt)+NaO_{0.5}(melt)+0.25O_2(gas) = AuSNa(melt)+FeO(melt), \quad (3)$$

$$Au(metal)+FeS(melt)+H_2O(melt) = AuHS(melt)+FeO(melt)+0.5H_2(gas), \quad (4)$$

where Me is a network modifier metal in the silicate melt, and Na can also be replaced by K in reaction (3).

In the experiments containing Cl but no S, Au can be dissolved in AuCl in addition to $AuO_{0.5}$ (reaction (2)); as shown in Table 3 and Figure 2, the addition of Cl can enhance the solubility of Au. A previous study has shown that the solubility of Au can be increased by 1 to 2 times when approximately 0.4 wt% Cl is added to the starting materials (Sullivan et al., 2018). However, we added 10–20 wt% NaCl to four of our experiments, and the results showed that NaCl did not significantly increase the solubility of Au (Appendix Table S1), indicating that the complexation of Au with Cl in magma is limited and much less than the effect of S.

Compared with Cl, S can substantially increase the solubility of Au in magma (Table 3 and Figure 2). Therefore, among recent high-pressure and high-temperature experimental studies, a large number focused on the effect of S on Au solubility in magma (Botcharnikov et al., 2010, 2011; Jégo et al., 2010, 2016; Zajacz et al., 2010, 2012, 2013; Jégo and Pichavant, 2012; Li and Audétat, 2013; Li et al., 2019; Sullivan et al., 2018). The experimental results showed that the Au solubility increased with increasing reduced S species in the silicate melts, but the trends were different for different redox conditions (Figure 3):

(1) Under reduced conditions (fO_2<~FMQ), all S in the silicate melts is in the form of reduced S species (S^{2-} and HS^-) (Jugo et al., 2010; Matjuschkin et al., 2016; Nash et al., 2019). Although the S solubility was found to be low in silicate melts, the Au content increased with increasing S content, indicating complexation of reduced S species with Au (reactions (3) and (4)).

(2) Under intermediate oxidized conditions (fO_2=~FMQ +2), the S solubility is much higher than that under reduced conditions, but the Au content does not simultaneously increase equally, indicating that the elevated S content of silicate melts under such redox conditions can be attributed to S^{6+}, which does not bind with Au. In our experiments under intermediate oxidized conditions, sulfide remained stable, indicating that S^{2-} and S^{6+} coexist in the melts. Therefore, the existence of S_3^- in silicate melts could be ruled out because no substantial increase in Au solubility was observed.

(3) Under highly oxidized conditions (fO_2=~FMQ+4.4), in silicate melts sulfide is not stable, whereas sulfate is. Under such conditions, the S content of silicate melts is high, but the Au solubility is very low, consistent with the Au solubility in previous S-free experiments, indicating that all S in silicate melts occurs as S^{6+} and Au as $AuO_{0.5}$ dissolved in the melts

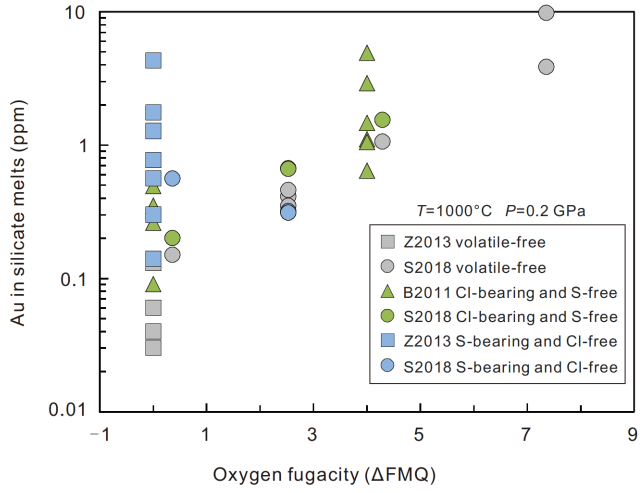

Figure 2 Solubility of Au in silicate melts as a function of oxygen fugacity and Cl and S content. The experiments were performed at 1000°C and 0.2 GPa (see Table 3 for more details on the experimental conditions). The addition of Cl and S increases the solubility of Au compared with that of the volatile-free experiments. Under reduced conditions (<FMQ+1), the addition of reduced S species is more efficient than Cl in increasing the solubility of Au in silicate melts. Under oxidized conditions (~FMQ+3), the addition of oxidized S species does not increase the solubility of Au, indicating that Au occurs only as $AuO_{0.5}$ or AuCl at high oxygen fugacities. Experimental data Z2013: Zajacz et al. (2013); S2018: Sullivan et al. (2018); B2011: Bell et al. (2011).

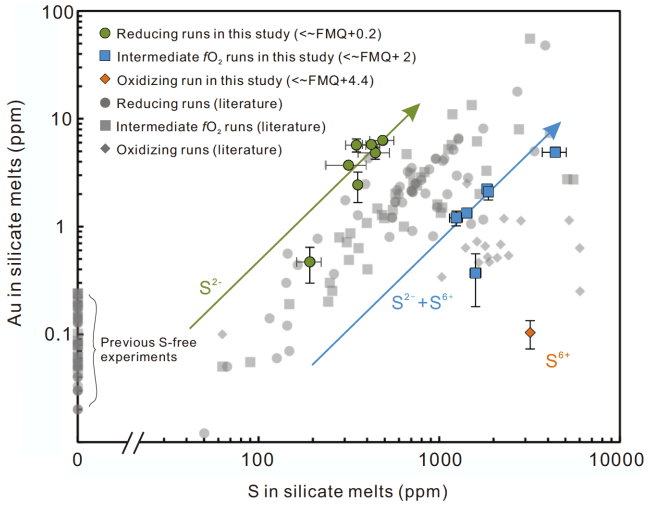

Figure 3 Solubility of Au in silicate melt as a function of S content. Because the solubility of Au in silicate melts is controlled by the reduced S species content (green dots), the solubility of Au in the S-bearing experiments is significantly higher than that in the S-free experiments. When S^{2-} and S^{6+} coexist, the S content of silicate melts is higher compared to that when only S^{2-} occurs, but the solubility of Au is not enhanced simultaneously (blue square), indicating that there is no intermediate valence S that binds with Au in silicate melts (such as S_3^-). When S^{6+} is the only S species in silicate melts (e.g., orange diamond), Au is dissolved only as $AuO_{0.5}$, which is consistent with the solubility of Au in previous S-free experiments. The trend lines in the figure are used to guide the eyes. The experimental data in this study are from Appendix Table S1 (1.0 GPa, 950°C) and the previous experimental data are from Botcharnikov et al. (2011); Jégo and Pichavant (2012); Jégo et al. (2010, 2016); Li et al. (2019); and Zajacz et al. (2013). Previous experiments were conducted in the pressure range of 0.2 to 3.0 GPa and temperature range of 800 to 1090°C, but mostly between 950 to 1050°C (Table 3). Since the valence state of S is temperature and pressure dependent, the previous reducing and oxidizing runs in the figure refer to the experiments with only S^{2-} and S^{6+} present, respectively, while the intermediate fO_2 runs refer to the experiments with coexisting S^{2-} and S^{6+}. The compositions of the silicate melts in previous experiments range from basaltic to rhyolitic.

(reaction (1)).

Previous experiments suggested that the solubility of Au in silicate melts may be controlled by fS_2, fH_2S, and fO_2 (Botcharnikov et al., 2011; Jégo and Pichavant, 2012; Jégo et al., 2016). In fact, the roles of fO_2 and fS_2 can be explained by the reduced S species content in the silicate melt. The amount of reduced S species in silicate melts is controlled by fS_2 and fO_2 and the FeO content of the melt, as shown in the following reaction (Smythe et al., 2017):

$$O^{2-}(\text{melt})+0.5S_2(\text{gas})=S^{2-}(\text{melt})+0.5O_2(\text{gas}), \quad (5)$$

The reduced S species content in silicate melts is positively correlated with fS_2/fO_2, suggesting that the solubility of Au may be directly controlled by the content of reduced S (Li et al., 2019). In contrast, the content of reduced S decreased with increasing fS_2/fO_2 in our experiments under reduced conditions (Appendix Figure S1). This was because the sulfide solubility of the Fe-poor silicate melts can be explained by the following reaction (Baker and Moretti, 2011):

$$4\text{FeS(sulfide)}+2O^{2-}(\text{melt})+O_2 = 2S^{2-}(\text{melt})+S_2+4\text{FeO(melt)}. \quad (6)$$

As shown in Appendix Figure S1, the S content gradually deviated from the trend line as the FeO content of the silicate melt increased in our H_2O-rich experiments, suggesting a shift in the S dissolution mechanism from reaction (6) to reaction (5). However, regardless of the FeO content of the melts, or even whether the sulfide is saturated, the Au content in the silicate melts increased with increasing S content (Figure 3), indicating that the solubility of Au is directly controlled by the content of the reduced S species in silicate melts instead of fS_2 or fO_2, which are only two of the factors influencing the S solubility. Therefore, we can infer that the conditions favorable for an increase in the content of the reduced S species in magma are favorable for the generation of Au-rich magma.

4. Generation of Au-rich magma and implications for the genesis of decratonic Au deposits in the North China Craton

4.1 Metallogenic model of decratonic Au deposits in the North China Craton

Gold deposits in the Liaodong and Jiaodong regions of the North China Craton are the most important Au deposits in China, with reserves of more than 4000–5000 tons (Yang et

al., 2003; Goldfarb and Santosh, 2014; Zhu et al., 2015; Groves and Santosh, 2016). Although the deposits are hosted in the margin of the ancient craton, they were mostly formed during the Early Cretaceous (130–120 Ma), suggesting that their genesis may not be related to orogenesis during cratonization. The age of Au mineralization coincides with the peak of the North China Craton destruction, and thus these deposits are considered to be "decratonic Au deposits" associated with magmatic-hydrothermal fluids (Zhu et al., 2015). Recent research suggests that the Au and volatiles of the decratonic Au deposits in the North China Craton may have been mainly derived from fertile mantle (Wang et al., 2020, 2021). At approximately 130–120 Ma, the North China Craton was affected by the subduction of the western paleo-Pacific plate and dehydration of the stagnant slab in the mantle transition zone, which led to the destruction and thinning of the craton and induced partial melting of the fertile mantle to produce Au-rich basalts (Zhu et al., 2012, 2015; Wang et al., 2020). These magmas ascended and evolved into intermediate to felsic magmas, eventually saturated with Au-rich fluids, and precipitated at shallow mineralization sites (Sun et al., 2007; Fan et al., 2011; Li et al., 2012a, 2012b; Zhu et al., 2015; Zheng et al., 2019). Therefore, revealing the physicochemical conditions that enhance the Au content in magmas allows us to better understand the genesis of decratonic Au deposits.

4.2 Moderately oxidized conditions favor the transport of Au and S

The ore-forming elements and fluids of decratonic Au deposits originated from mantle-derived magmas (Zhu et al., 2015). Because mantle sulfides are the major Au-bearing minerals, it is believed that high fO_2 conditions are necessary to convert sulfides to Au-free sulfates in order to completely destroy the sulfides and release Au (e.g., Mungall, 2002). In fact, it is difficult to completely consume sulfide in this case. Recent experiments have demonstrated that increasing pressure and decreasing temperature can stabilize sulfides at higher fO_2 (Matjuschkin et al., 2016; Nash et al., 2019), suggesting that complete sulfide conversion to sulfate is unlikely under lower crustal conditions, even if the fO_2 of magma exceeds FMQ+3. The subduction zone is considered an oxidized environment, and the fO_2 of primitive arc basalt ranges from FMQ+0.5 to FMQ+2, and locally up to or above FMQ+3 (Frost and McCammon, 2008; Richards, 2015; Wang et al., 2019, 2020). Thus, it is difficult to exceed FMQ +3 in the source of decratonic Au deposits. On the other hand, the amount of garnet increases with depth in the thick cratonic lithosphere (although the lithospheric thickness of the decratonic Au deposits in the North China Craton has been thinned, it remains 50–70 km in Jiaodong), and the increase in garnet will reduce the fO_2 (Wood et al., 2013). Therefore, magmatism in the source of decratonic Au deposits may not completely exhaust the sulfides.

Considering that sulfide is the major host of Au, if it is saturated during magmatic processes, it may play a role in Au pre-enrichment, which would have a positive impact on subsequent mineralization processes (Botcharnikov et al., 2011; Audétat and Simon, 2012; Xiong et al., 2020). Recent studies have shown that as the solubility of Au in magma increases, the partition coefficient between sulfide (monosulfide solid solution, MSS) and magma decreases, to as low as 10 (Li et al., 2019). This means that a small amount of residual sulfide in the source or during magmatic processes does not necessarily result in depletion of Au in the magma. The key to the formation of Au-rich magma is to form a reduced S species-rich magma if sulfides are present.

In general, excessively high or low fO_2 hinder the formation of Au-rich magma during partial melting of the mantle or fractional crystallization of basalts in the source. All sulfides (S^{2-}) will be converted to sulfates (S^{6+}) under highly oxidized conditions, which in turn results in very low Au solubility in the magma (Figure 3), making it difficult to provide adequate Au for subsequent exsolved fluids. On the other hand, the amount of reduced S decreases with fO_2, and the Au content in the magma decreases under very reduced conditions (reaction (3)). Moreover, low fO_2 suppresses the presence of intermediate valence S or the subsequent exsolution of S_3^--rich fluid, which greatly enhances the ability of fluids to extract Au from the magma (Pokrovski et al., 2013). Therefore, moderately oxidized conditions favor Au migration from the mantle source region to the upper crust for mineralization. In addition, the formation of large Au deposits requires not only massive amounts of Au but also substantial S (Li et al., 2012a). Moderately oxidized conditions promote the coexistence of S^{2-} and S^{6+} in the magma, which not only maintains the transport capacity of Au (no reduction in S^{2-} content), but also increases the transport capacity of S (higher solubility of S^{6+} in the magma). As shown in Figure 3, maximizing the solubility of Au and S in the magma at the same time under moderately oxidized conditions is favorable.

The age of the decratonic Au deposits in the North China Craton coincides with the thinning stage of the North China Craton destruction. Craton thinning is controlled by dehydration of the stagnant slab in the mantle transition zone (Zhu et al., 2012; Xu et al., 2018). The engagement of these deep melts and fluids and the thinning of the North China Craton both elevate the fO_2 in the source region. Because the content of reduced S increases with increasing temperature and decreasing pressure (Smythe et al., 2017), the strong extensional tectonic setting of the Early Cretaceous North China Craton may have provided favorable conditions for the rapid ascent of mantle-derived melts and fluids, facilitating the transport of Au and S.

4.3 High-pressure and H_2O-rich conditions favor Au and S transport

Recent S solubility experiments suggest that increasing the H_2O content of magma can increase both sulfide and sulfate solubility (Fortin et al., 2015; Zajacz and Tsay, 2019; Liu et al., 2021; Liu X et al., 2020). The formation of H_2O-rich magmas requires H_2O-rich sources and high pressure (H_2O solubility in magma is generally controlled by pressure; Keppler, 2013). Both conditions are well met for the source of decratonic Au deposits in the North China Craton, as the dehydration of the western paleo-Pacific stagnant plate in the mantle transition zone can provide large amounts of H_2O (Liu et al., 2018, 2019). Furthermore, the thinned craton can provide over 1.5 GPa pressure (50 km thickness, Xiong et al., 2011), which promotes the generation of H_2O-rich magmas.

Pressure affects not only the solubility of H_2O in the magma, but also the transport of Au and S. Under high-pressure conditions, the sulfide is MSS, which has a lower $D_{Au}^{sulfide/magma}$ than liquid sulfide, implying that sulfide residues in the source may not result in depletion of Au in magmas (Li et al., 2019). As the pressure increases, the partition coefficient of S between the fluid and melt decreases from several hundred to less than 10 (Binder et al., 2018; Colin et al., 2020), indicating that the partition coefficient may decrease to 1 when the pressure increases to a certain level, at which point the H_2O-rich magma may have a similar capacity to transport S as the fluid. It is also possible to form supercritical fluids at high pressures (Ni et al., 2017; Ni, 2020; Xiong et al., 2020). Considering the stability of S_3^- in fluids, supercritical fluids will probably have very high solubility of Au and S and excellent migration ability. However, studies on the formation conditions and geochemical properties of supercritical fluids are still scarce, especially on *in situ* high-pressure experiments.

In summary, Au-rich mantle-derived magmas may have the following features: (1) moderately oxidized (~FMQ+2 or an fO_2 range of sulfide and sulfate coexistence), which can increase the solubility of S and Au simultaneously; (2) H_2O-rich, which increases the S solubility and also provides a large quantity of H_2O for subsequent fluid exsolution. In addition, if the initial magma is highly hydrous, it is possible that the evolved magma will reach fluid saturation in the lower crust. Considering the high $D_{Au}^{fluid/silicate\ melt}$ and $D_{S}^{fluid/silicate\ melt}$, these exsolved fluids will directly extract and transport large amounts of Au and S. It should be noted that the formation of Au deposits, especially large and giant Au deposits, involves numerous complex processes that are affected by many factors and may require various favorable conditions, including favorable tectonic settings and the formation and smooth migration and precipitation of ore-forming element-rich melts and fluids (Richards, 2013). In this paper, we constrain the physicochemical conditions favorable for the generation and migration of Au-rich magma during the ore formation of decratonic Au deposits in the North China Craton only in terms of Au solubility and melt and fluid partitioning experiments. Our model has yet to be verified by future investigations based on natural samples.

5. Conclusions and outlook

In this paper, we reviewed the valence and species of Au, the fluid/melt partitioning of Au, the solubility of Au in magma, and the controlling factors of magma-hydrothermal Au deposit formation:

(1) The contents of Au in mantle-derived basalts and intermediate to felsic magmas derived from subsequent fractional crystallization processes are controlled by the content of reduced S species (S^{2-} and HS^-) in the magma.

(2) If the source region is moderately oxidized (fO_2=~FMQ+2), it will be more favorable for transporting Au and S. On the one hand, intermediate fO_2 promotes the solubility of reduced S species, which enhances the solubility of Au. On the other hand, intermediate fO_2 favors the stability of intermediate valence S (e.g., S_3^-) and S^{6+}. S_3^- facilitates efficient extraction of Au from magma during fluid exsolution, and S^{6+} the transport of large amounts of S required for mineralization.

(3) The formation of H_2O-rich magma further increases the S solubility of the magma, thus increasing the ability of the magma to transport Au. The formation of H_2O-rich magma also provides adequate H_2O for fluid exsolution at an early stage. The fluid exsolution further enriches S and Au in the magma.

(4) During fluid evolution, Au mainly binds with S_3^- or HS^- during migration at the high-temperature stage, and $AuCl_2^-$ is probably the major complexation as the temperature decreases.

Although we summarize the physicochemical conditions favorable for Au enrichment and migration during the formation of magmatic-hydrothermal deposits, many deep processes are still unclear regarding the transport of large amounts of Au in the North China Craton, and relevant high-pressure and high-temperature experiments are still relatively lacking. We suggest that future research should focus on: (1) the formation conditions of supercritical fluids and their effects on Au and S transport; (2) whether fluids can be saturated under high-pressure conditions (such as lower crustal conditions) and their roles, and (3) the partition coefficients of Au and S between fluids and silicate melts and sulfides under various redox conditions and the effects of volatiles under high-pressure conditions.

Acknowledgements *We thank three anonymous reviewers and the responsible editor for their constructive comments and Changming Xing for discussion. This work was supported by the National Key Research and Development Project of China (Grant No. 2016YFC0600104), the National Natural Science Foundation of China (Grant No. 41573053) and the Youth Innovation Promotion Association CAS (Grant No. 2019344).*

References

Audétat A. 2019. The metal content of magmatic-hydrothermal fluids and its relationship to mineralization potential. Econ Geol, 114: 1033–1056
Audétat A, Simon A C. 2012. Magmatic controls on porphyry copper genesis. Soc Econ Geol Spec Publ, 16: 553–572
Audétat A, Lowenstern J B. 2014. Melt inclusions. In: Holland H D, Turekian K K, eds. Treatise on Geochemistry. 2 ed. 13: 143–173
Baker D R, Moretti R. 2011. Modeling the solubility of sulfur in magmas: A 50-year old geochemical challenge. Rev Mineral Geochem, 73: 167–213
Bell A S, Simon A, Guillong M. 2009. Experimental constraints on Pt, Pd and Au partitioning and fractionation in silicate melt -sulfide -oxide -aqueous fluid systems at 800°C, 150 MPa and variable sulfur fugacity. Geochim Cosmochim Acta, 73: 5778–5792
Bell A S, Simon A, Guillong M. 2011. Gold solubility in oxidized and reduced, water-saturated mafic melt. Geochim Cosmochim Acta, 75: 1718–1732
Binder B, Wenzel T, Keppler H. 2018. The partitioning of sulfur between multicomponent aqueous fluids and felsic melts. Contrib Mineral Petrol, 173: 18
Bodnar R J, Lecumberri-Sanchez P, Moncada D, Steele-Macinnis M. 2014. Fluid inclusions in hydrothermal ore deposit. In: Holland H D, Turekian K K, eds. Treatise on Geochemistry. 2 ed. 119–142
Borisov A, Palme H. 1996. Experimental determination of the solubility of Au in silicate melts. Mineral Petrol, 56: 297–312
Botcharnikov R E, Linnen R L, Holtz F. 2010. Solubility of Au in Cl- and S-bearing hydrous silicate melts. Geochim Cosmochim Acta, 74: 2396–2411
Botcharnikov R E, Linnen R L, Wilke M, Holtz F, Jugo P J, Berndt J. 2011. High gold concentrations in sulphide-bearing magma under oxidizing conditions. Nat Geosci, 4: 112–115
Brenan J M, Bennett N R, Zajacz Z. 2016. Experimental results on fractionation of the highly siderophile elements (HSE) at variable pressures and temperatures during planetary and magmatic differentiation. Rev Mineral Geochem, 81: 1–87
Brugger J, Liu W, Etschmann B, Mei Y, Sherman D M, Testemale D. 2016. A review of the coordination chemistry of hydrothermal systems, or do coordination changes make ore deposits? Chem Geol, 447: 219–253
Chen Y, Pirajno F, Li N, Guo D, Lai Y. 2009. Isotope systematics and fluid inclusion studies of the Qiyugou breccia pipe-hosted gold deposit, Qinling Orogen, Henan province, China: Implications for ore genesis. Ore Geol Rev, 35: 245–261
Colin A, Schmidt C, Pokrovski G S, Wilke M, Borisova A Y, Toplis M J. 2020. *In situ* determination of sulfur speciation and partitioning in aqueous fluid-silicate melt systems. Geochem Persp Let, Let: 31–35
Fan H R, Hu F F, Wilde S A, Yang K F, Jin C W. 2011. The Qiyugou gold-bearing breccia pipes, Xiong'ershan region, central China: Fluid-inclusion and stable-isotope evidence for an origin from magmatic fluids. Int Geol Rev, 53: 25–45
Fortin M A, Riddle J, Desjardins-Langlais Y, Baker D R. 2015. The effect of water on the sulfur concentration at sulfide saturation (SCSS) in natural melts. Geochim Cosmochim Acta, 160: 100–116
Frost D J, McCammon C A. 2008. The redox state of Earth's mantle. Annu Rev Earth Planet Sci, 36: 389–420
Frank M R, Candela P A, Piccoli P M, Glascock M D. 2002. Gold solubility, speciation, and partitioning as a function of HCl in the brine-silicate melt-metallic gold system at 800°C and 100 MPa. Geochim Cosmochim Acta, 66: 3719–3732
Goldfarb R J, Santosh M. 2014. The dilemma of the Jiaodong gold deposits: Are they unique? Geosci Front, 5: 139–153
Groves D I, Santosh M. 2016. The giant Jiaodong gold province: The key to a unified model for orogenic gold deposits? Geosci Front, 7: 409–417
Hanley J J, Pettke T, Mungall J E, Spooner E T C. 2005. The solubility of platinum and gold in NaCl brines at 1.5 kbar, 600 to 800°C: A laser ablation ICP-MS pilot study of synthetic fluid inclusions. Geochim Cosmochim Acta, 69: 2593–2611
Heinrich C A, Candela P A. 2014. Fluids and ore formation in the Earth's crust. In: Holland H D, Turekian K K, eds. Treatise on Geochemistry. 2 ed. 1–28
von der Heyden B P. 2020. Shedding light on ore deposits: A review of synchrotron X-ray radiation use in ore geology research. Ore Geol Rev, 117: 103328
Jégo S, Pichavant M, Mavrogenes J A. 2010. Controls on gold solubility in arc magmas: An experimental study at 1000°C and 4 kbar. Geochim Cosmochim Acta, 74: 2165–2189
Jégo S, Pichavant M. 2012. Gold solubility in arc magmas: Experimental determination of the effect of sulfur at 1000°C and 0.4 GPa. Geochim Cosmochim Acta, 84: 560–592
Jégo S, Nakamura M, Kimura J I, Iizuka Y, Chang Q, Zellmer G F. 2016. Is gold solubility subject to pressure variations in ascending arc magmas? Geochim Cosmochim Acta, 188: 224–243
Jugo P J, Wilke M, Botcharnikov R E. 2010. Sulfur K-edge XANES analysis of natural and synthetic basaltic glasses: Implications for S speciation and S content as function of oxygen fugacity. Geochim Cosmochim Acta, 74: 5926–5938
Keppler H. 2013. Volatiles under high pressure. In: Karato S, ed. Physics and Chemistry of the Deep Earth. Hoboken: Wiley Blackwell. 3–37
Kiseeva E S, Fonseca R O C, Smythe D J. 2017. Chalcophile elements and sulfides in the upper mantle. Elements, 13: 111–116
Li J W, Bi S J, Selby D, Chen L, Vasconcelos P, Thiede D, Zhou M F, Zhao X F, Li Z K, Qiu H N. 2012a. Giant Mesozoic gold provinces related to the destruction of the North China craton. Earth Planet Sci Lett, 349-350: 26–37
Li J W, Li Z K, Zhou M F, Chen L, Bi S J, Deng X D, Qiu H N, Cohen B, Selby D, Zhao X F. 2012b. The Early Cretaceous Yangzhaiyu Lode gold deposit, North China Craton: A link between craton reactivation and gold veining. Econ Geol, 107: 43–79
Li Y, Audétat A. 2013. Gold solubility and partitioning between sulfide liquid, monosulfide solid solution and hydrous mantle melts: Implications for the formation of Au-rich magmas and crust–mantle differentiation. Geochim Cosmochim Acta, 118: 247–262
Li Y, Feng L, Kiseeva E S, Gao Z, Guo H, Du Z, Wang F, Shi L. 2019. An essential role for sulfur in sulfide-silicate melt partitioning of gold and magmatic gold transport at subduction settings. Earth Planet Sci Lett, 528: 115850
Liu W, Etschmann B, Testemale D, Hazemann J L, Rempel K, Müller H, Brugger J. 2014. Gold transport in hydrothermal fluids: Competition among the Cl^-, Br^-, HS^- and NH_3(aq) ligands. Chem Geol, 376: 11–19
Liu X, Matsukage K N, Li Y, Takahashi E, Suzuki T, Xiong X. 2018. Aqueous fluid connectivity in subducting oceanic crust at the mantle transition zone conditions. J Geophys Res-Solid Earth, 123: 6562–6573
Liu X, Matsukage K N, Nishihara Y, Suzuki T, Takahashi E. 2019. Stability of the hydrous phases of Al-rich phase D and Al-rich phase H in deep subducted oceanic crust. Am Miner, 104: 64–72
Liu K, Zhang L, Guo X, Ni H. 2021. Effects of sulfide composition and melt H_2O on sulfur content at sulfide saturation in basaltic melts. Chem Geol, 559: 119913
Liu X, Xu T, Xiong X. 2020. High sulfur solubility in hydrous felsic magma at coexistence of sulfide and sulfate. Goldschmidt Conference, doi: 10.46427/gold2020.1615
Loucks R R, Mavrogenes J A. 1999. Gold solubility in supercritical hydrothermal brines measured in synthetic fluid inclusions. Science, 284: 2159–2163
Mao J, Goldfarb R, Zhang Z, Xu W, Qiu Y, Deng J. 2002. Gold deposits in the Xiaoqinling-Xiong'ershan region, Qinling Mountains, central China. Miner Depos, 37: 306–325
Matjuschkin V, Blundy J D, Brooker R A. 2016. The effect of pressure on sulphur speciation in mid- to deep-crustal arc magmas and implications

for the formation of porphyry copper deposits. Contrib Mineral Petrol, 171: 66
Mungall J E. 2002. Roasting the mantle: Slab melting and the genesis of major Au and Au-rich Cu deposits. Geology, 30: 915–918
Nash W M, Smythe D J, Wood B J. 2019. Compositional and temperature effects on sulfur speciation and solubility in silicate melts. Earth Planet Sci Lett, 507: 187–198
Ni H. 2020. Properties and effects of supercritical geofluids (in Chinese with English abstract). Bull Mineral Petrol Geochem, 39: 443–447
Ni H, Zhang L, Xiong X, Mao Z, Wang J. 2017. Supercritical fluids at subduction zones: Evidence, formation condition, and physicochemical properties. Earth-Sci Rev, 167: 62–71
Pearson R G. 1963. Hard and soft acids and bases, HSAB, Fundamental principles. J Am Chem Soc, 85: 581–587
Pettke T, Oberli F, Audétat A, Guillong M, Simon A C, Hanley J J, Klemm L M. 2012. Recent developments in element concentration and isotope ratio analysis of individual fluid inclusions by laser ablation single and multiple collector ICP-MS. Ore Geol Rev, 44: 10–38
Pokrovski G S, Tagirov B R, Schott J, Hazemann J L, Proux O. 2009. A new view on gold speciation in sulfur-bearing hydrothermal fluids from *in situ* X-ray absorption spectroscopy and quantum-chemical modeling. Geochim Cosmochim Acta, 73: 5406–5427
Pokrovski G S, Dubrovinsky L S. 2011. The S_3^- ion is stable in geological fluids at elevated temperatures and pressures. Science, 331: 1052–1054
Pokrovski G S, Borisova A Y, Bychkov A Y. 2013. Speciation and transport of metals and metalloids in geological vapors. Rev Mineral Geochem, 76: 165–218
Pokrovski G S, Kokh M A, Guillaume D, Borisova A Y, Gisquet P, Hazemann J L, Lahera E, Del Net W, Proux O, Testemale D, Haigis V, Jonchière R, Seitsonen A P, Ferlat G, Vuilleumier R, Saitta A M, Boiron M C, Dubessy J. 2015. Sulfur radical species form gold deposits on Earth. Proc Natl Acad Sci USA, 112: 13484–13489
Richards J P. 2013. Giant ore deposits formed by optimal alignments and combinations of geological processes. Nat Geosci, 6: 911–916
Richards J P. 2015. The oxidation state, and sulfur and Cu contents of arc magmas: Implications for metallogeny. Lithos, 233: 27–45
Seo J H, Guillong M, Heinrich C A. 2009. The role of sulfur in the formation of magmatic-hydrothermal copper-gold deposits. Earth Planet Sci Lett, 282: 323–328
Seward T M. 1973. Thio complexes of gold and the transport of gold in hydrothermal ore solutions. Geochim Cosmochim Acta, 37: 379–399
Seward T M, Williamsjones A E, Migdisov A A. 2014. The chemistry of metal transport and deposition by ore-forming hydrothermal fluids. In: Holland H D, Turekian K K, eds. Treatise on Geochemistry. 2 ed. 29–57
Simon A C, Pettke T, Candela P A, Piccoli P M, Heinrich C A. 2003. Experimental determination of Au solubility in rhyolite melt and magnetite: Constraints on magmatic Au budgets. Am Miner, 88: 1644–1651
Simon A C, Frank M R, Pettke T, Candela P A, Piccoli P M, Heinrich C A. 2005. Gold partitioning in melt-vapor-brine systems. Geochim Cosmochim Acta, 69: 3321–3335
Simon A C, Pettke T, Candela P A, Piccoli P M, Heinrich C A. 2007. The partitioning behavior of As and Au in S-free and S-bearing magmatic assemblages. Geochim Cosmochim Acta, 71: 1764–1782
Smythe D J, Wood B J, Kiseeva E S. 2017. The S content of silicate melts at sulfide saturation: New experiments and a model incorporating the effects of sulfide composition. Am Miner, 102: 795–803
Sullivan N A, Zajacz Z, Brenan J M. 2018. The solubility of Pd and Au in hydrous intermediate silicate melts: The effect of oxygen fugacity and the addition of Cl and S. Geochim Cosmochim Acta, 231: 15–29
Sun W, Ding X, Hu Y H, Li X H. 2007. The golden transformation of the Cretaceous plate subduction in the west Pacific. Earth Planet Sci Lett, 262: 533–542
Sun X, Zhang Y, Xiong D, Sun W, Shi G, Zhai W, Wang S. 2009. Crust and mantle contributions to gold-forming process at the Daping deposit, Ailaoshan gold belt, Yunnan, China. Ore Geol Rev, 36: 235–249
Walshe J L, Cleverley J S. 2009. Gold deposits: Where, when and why. Elements, 5: 288
Wang J, Xiong X, Chen Y, Huang F. 2020. Redox processes in subduction zones: Progress and prospect. Sci China Earth Sci, 63: 1952–1968
Wang J, Xiong X, Takahashi E, Zhang L, Li L, Liu X. 2019. Oxidation state of arc mantle revealed by partitioning of V, Sc, and Ti between mantle minerals and basaltic melts. J Geophys Res-Solid Earth, 124: 4617–4638
Wang Z, Cheng H, Zong K, Geng X, Liu Y, Yang J, Wu F, Becker H, Foley S, Wang C Y. 2020. Metasomatized lithospheric mantle for Mesozoic giant gold deposits in the North China Craton. Geology, 48: 169–173
Wang Z, Xu Z, Cheng H, Zou Y, Guo J, Liu Y, Yang J, Zong K, Xiong L, Hu Z. 2021. Precambrian metamorphic crustal basement cannot provide much gold to form giant gold deposits in the Jiaodong Peninsula, China. Precambrian Res, 354: 106045
Williams-Jones A E, Bowell R J, Migdisov A A. 2009. Gold in solution. Elements, 5: 281–287
Wood B J, Kiseeva E S, Matzen A K. 2013. Garnet in the Earth's mantle. Elements, 9: 421–426
Xiong X L, Liu X C, Zhu Z M, Li Y, Xiao W S, Song M S, Zhang S, Wu J H. 2011. Adakitic rocks and destruction of the North China Craton: Evidence from experimental petrology and geochemistry. Sci China Earth Sci, 54: 858–870
Xiong X, Liu X, Li L, Wang J, Chen W, Ruan M, Xu T, Sun Z, Huang F, Li J, Zhang L. 2020. The partitioning behavior of trace elements in subduction zones: Advances and prospects. Sci China Earth Sci, 63: 1938–1951
Xu Y, Li H, Hong L, Ma L, Ma Q, Sun M. 2018. Generation of Cenozoic intraplate basalts in the big mantle wedge under eastern Asia. Sci China Earth Sci, 61: 869–886
Yang J H, Wu F Y, Wilde S A. 2003. A review of the geodynamic setting of large-scale Late Mesozoic gold mineralization in the North China Craton: An association with lithospheric thinning. Ore Geol Rev, 23: 125–152
Zajacz Z, Seo J H, Candela P A, Piccoli P M, Heinrich C A, Guillong M. 2010. Alkali metals control the release of gold from volatile-rich magmas. Earth Planet Sci Lett, 297: 50–56
Zajacz Z, Candela P A, Piccoli P M, Wälle M, Sanchez-Valle C. 2012. Gold and copper in volatile saturated mafic to intermediate magmas: Solubilities, partitioning, and implications for ore deposit formation. Geochim Cosmochim Acta, 91: 140–159
Zajacz Z, Candela P A, Piccoli P M, Sanchez-Valle C, Wälle M. 2013. Solubility and partitioning behavior of Au, Cu, Ag and reduced S in magmas. Geochim Cosmochim Acta, 112: 288–304
Zajacz Z, Tsay A. 2019. An accurate model to predict sulfur concentration at anhydrite saturation in silicate melts. Geochim Cosmochim Acta, 261: 288–304
Zheng Y, Mao J, Chen Y, Sun W, Ni P, Yang X. 2019. Hydrothermal ore deposits in collisional orogens. Sci Bull, 64: 205–212
Zhu R X, Xu Y G, Zhu G, Zhang H F, Xia Q K, Zheng T Y. 2012. Destruction of the North China Craton. Sci China Earth Sci, 55: 1565–1587
Zhu R X, Fan H R, Li J W, Meng Q R, Li S R, Zeng Q D. 2015. Decratonic gold deposits. Sci China Earth Sci, 58: 1523–1537

(Responsible editor: Huaiwei NI)